

Ultra-Fast Click Modification of Self-Assembled Zwitterionic Copolymer Membranes for Enhanced Ion Selectivity

Abhishek N. Mondal, Samuel J. Lounder, Luca Mazzaferro, and Ayse Asatekin*

Membranes that can separate small molecules and ions are of immense interest in various separations. Self-assembling zwitterionic amphiphilic copolymers (ZACs) are extremely promising as exceptionally fouling-resistant membrane selective layers with narrow size cut-offs. However, it is difficult to tune their effective pore size within time frames compatible with roll-to-roll manufacturing. We report a novel, ultra-fast approach for tuning the pore size of ZAC-based membranes through thiol-ene click chemistry that brings the needed post-modification time from tens of minutes to only 10-40 s, making its integration feasible in large scale manufacturing systems. Resultant membranes have enhanced organic molecule and salt rejections, resulting in tunable mono-/divalent ion selectivity. For instance, cross-linking increases Na₂SO₄ rejections from <20% to up to 83%, while NaCl rejection remains below 30%. Furthermore, these membranes completely resist fouling by oil and proteins, outperforming commercial membranes. These results suggest that our cross-linked membranes have the potential to be used in separations in the food industry, pharmaceutical manufacturing, and wastewater treatment.

1. Introduction

Membrane separations are energy-efficient, scalable, portable, simple to operate, and require no added solvents, applicable to various sectors including pharmaceuticals, biological, desalination, food industry, and water treatment. [1–9] However, their broader use is often curtailed by limited selectivity and/or severe performance loss during operation due to fouling. [8,10,11] To broaden the applications where membranes are used, new and improved membrane materials that enable enhanced and customizable selectivity, high flux, and fouling resistance are needed. These novel membrane technologies should also be manufactured through scalable methods, and be resilient under realistic operating conditions. [8,9,11]

Membranes with tunable size-based selectivity between small molecules (1–2 nm) are of interest for many separations in the food industry, pharmaceutical manufacturing, textile dying and

A. N. Mondal, S. J. Lounder, L. Mazzaferro, A. Asatekin Department of Chemical and Biological Engineering Tufts University Medford, MA 02155, USA E-mail: ayse.asatekin@tufts.edu

The ORCID identification number(s) for the author(s) of this article can be found under https://doi.org/10.1002/admi.202102496.

DOI: 10.1002/admi.202102496

processing, and buffer exchange and purification of peptides.^[12–18] Nanofiltration (NF) membranes, defined by nominal pore diameters of ≈1-3 nm, are typically considered for these separations, even though their selectivity is complex, incorporating size, charge, and polarity effects.[19,20] NF membranes are typically thin film composite (TFC) membranes with cross-linked polyamide (PA) selective layers. While PA-TFC NF membranes are well-established in the industry, it is extremely difficult to control and tune their selectivity for specific separations. Their customization relies on empirical efforts and still offers limited capability in separating organic solutes.[21,22] In addition, the PA chemistry is inherently prone to Furthermore, they are highly prone to fouling by various components in feed water (e.g., biomacromolecules, oil).[8] Fouling management through regular cleaning and membrane replacement accounts for a significant portion of

capital and operating costs.[20,23,24] Therefore, there is an urgent need for the development of novel material systems that exhibit high and controllable selectivity in the ≈1 nm range and resist fouling. In addition, the scalability of manufacturing methods needs to be seriously considered in developing such new membrane materials. While many new membrane technologies with enhanced selectivity and/or fouling resistance have been reported in the scientific literature, many utilize techniques that are not easy to translate to roll-to-roll manufacturing such as multi-step processes (e.g., electroless deposition, chemical vapor deposition), long processing times (e.g., post-treatment or cross-linking reactions that require hours or even days), batch processes that are difficult to apply to large areas (e.g., spin coating), etc. Novel material chemistries for high selectivity and fouling resistance must, therefore, be designed to be incorporated into established membrane manufacturing techniques seamlessly. Importantly, for rollto-roll manufacturing, processing times must be extremely short, on the order of seconds.

Polymer self-assembly, which involves the spontaneous formation of nano-scale structures through intermolecular interactions, can be an efficient tool to provide membranes with controlled pore size, high selectivity, and scalability. Self-assembly and non-solvent induced phase separation (SNIPS) of block copolymers (BCPs) has been used to prepare asymmetric membranes with uniform pores and controlled pore functionality.^[25–27] Although SNIPS is highly scalable, ^[28,29] it is difficult to reach small pore sizes via BCP self-assembly.

Comb-shaped copolymers with hydrophobic backbones and polyethylene oxide (PEO) side chains can self-assemble to create fouling-resistant membranes with ≈1.5–2 nm effective pore sizes, [30,31] but the hydrolysis of the PEO side chains limits their use to neutral pH. Lyotropic liquid crystal (LLC) assemblies can achieve sub-nanometer, charged nanodomains that perform as promising reverse osmosis membranes, but their selectivity is not size selective due to their positively charged surfaces. They also require somewhat complex manufacturing with comparatively limited scalability. [32,33] Furthermore, it is extremely difficult to tune the effective pore size of comb-shaped copolymers and LLC-based membranes without synthesizing novel materials and optimizing their processing.

Our group has leveraged the self-assembly of random zwitterionic amphiphilic copolymers (ZACs) to form TFC membranes with ≈1.2–1.5 nm effective pore size and excellent fouling resistance. [20,23,24] Zwitterions, defined as molecules with equal numbers of positive and negative charges connected by covalent bonds, exhibit exceptional fouling resistance characteristics due to their high degree of hydration. [34] Many researchers have used this feature of zwitterionic groups to enhance fouling resistance by either modifying the membrane surface chemistry to attach zwitterionic moieties[35-37] or by coating membranes with zwitterionic hydrogels.^[38] Zwitterions are also extremely polar, which drives microphase separation in a variety of zwitterionic copolymer systems. [39,40] ZACs, random/statistical copolymers combining a hydrophobic monomer with a zwitterionic monomer, microphase separate to form bicontinuous networks of zwitterionic and hydrophobic domains over a broad copolymer composition range (Figure 1A). The zwitterionic domains, bound by the hydrophobic domains of the copolymer, act as a network of zwitterionic nanochannels that permeate water and solutes small enough to enter them (Figure 1A). Thin film composite (TFC) membranes can be easily fabricated by coating ZACs onto a porous substrate to form a selective layer. Membranes with ZAC selective layers possess unprecedented fouling resistance due to the zwitterionic groups, completely resisting fouling by a broad range of foulants including oil/water emulsions, proteins, and components found in surface water and wastewater effluents.[8,20,23]

The fouling resistance and small pore size make ZAC-based membranes exceptionally promising for treating wastewater streams, especially compared with ultrafiltration (UF) membranes commonly used in these applications. However, the effective pore size of these membranes is too large for most applications where NF membranes are used. As-prepared ZAC-based membranes exhibit minimal salt rejection over a range of hydrophobic and zwitterionic monomer chemistries. [20,23] Novel, scalable methods to tune the pore size of these membranes are needed to access important applications that require higher organics removal and mono-/divalent ion selectivity, including but not limited to waste water treatment, removal of small organic molecules, and water softening. Furthermore, adapting ZAC-based membranes to exhibit NF-like selectivity would enable us to circumvent major limitations arising from the inherent chemical structure of interfacially polymerized polyamide NF membranes, including chlorine sensitivity^[19,20] and fouling.^[19,20,23,41]

Post-functionalization is a common approach for tailoring the properties and functionality of membranes after nanostructure formation.^[42] This approach has previously been used to tune ion rejection and selectivity of membranes and to enhance fouling resistance.[42-45] However, in most common chemical reaction schemes used in lab-scale research, reaction rates are too low compared with time scales that are usable in large scale roll-to-roll membrane fabrication lines. For example, amineacyl halide coupling reactions used in the post-functionalization of polyamide reverse osmosis membranes require on the order of 5 min to complete, [45] while carbodiimide coupling reactions take up to 20 min. [44] We have recently shown that UV polymerization photo-cross-linking of cross-linkable random ZACs can lead to smaller effective pore sizes with divalent/ monovalent ion selectivity and complete resistance to irreversible fouling. However, this process also requires 5-20 min of UV exposure for sufficient cross-linking.[19,41] These time scales are not feasible in roll-to-roll systems, where residence times on the order of min are not possible within reasonable equipment sizes and operating parameters. Therefore, to truly impact large scale applications, post-fabrication techniques to tune and enhance membrane performance must occur in time scales measured

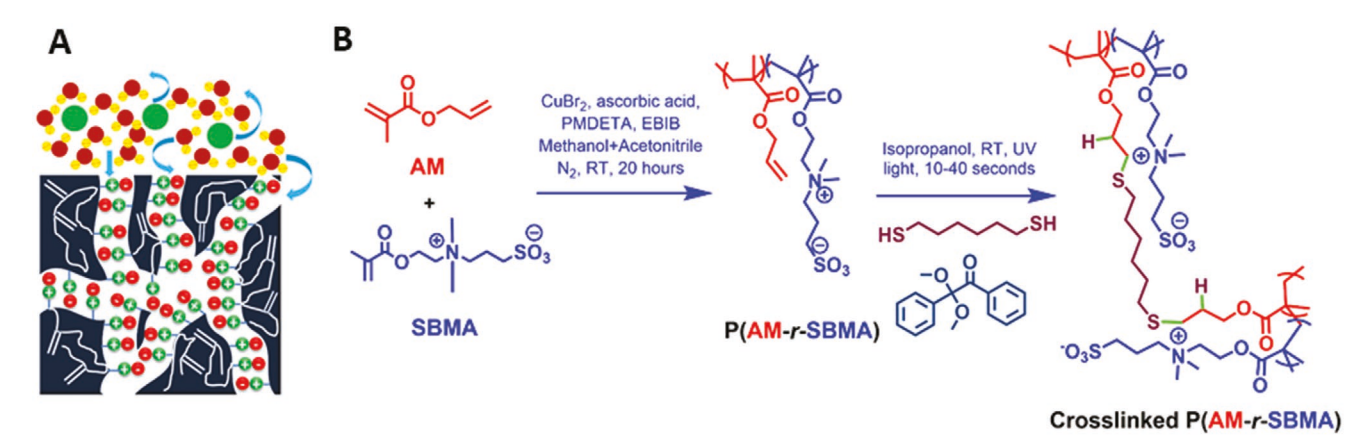


Figure 1. A) Schematic representation of self-assembly to generate bicontinuous networks of zwitterionic (shown with green and red charged groups) and cross-linkable hydrophobic (dark blue) domains. Water and small solutes can pass through the ZI domains. B) Synthesis scheme of a cross-linkable random zwitterionic copolymer (ZAC) and its cross-linking reaction through thiol-ene click chemistry.

in seconds, and are simple to apply and execute. This is also true for tuning the selectivity of ZAC-based membranes for approaching novel, NF-type separations.

In this work, we have identified thiol-ene "click" chemistry as a chemical approach for ultra-fast cross-linking of ZAC-based membranes to achieve tunable effective pore sizes that extend into the NF range, bringing processing times from ≈20 min down to 10s of seconds. Thiol-ene "click" chemistry is characterized by very high reaction rates, high conversions, and selective yields. These features make it a good choice for postfunctionalization of membranes in roll-to-roll systems, where short residence times with high yields are required. [46] To date, UV-initiated thiol-ene click chemistry has been used in polymer functionalization, dendrimer synthesis, or supramolecular catalysis.[46] This reaction has not been utilized as broadly in membrane functionalization. Studies report thiol-ene reactions for cross-linking or functionalization of ion exchange membranes, [47,48] proton exchange membranes, [49] hydrogel thin films,^[50] and cross-linked poly(ethylene glycol)/ionic liquid blend membranes for CO₂ separation.^[51] While each approach demonstrated some performance improvement, processing times were still too long for roll-to-roll manufacturing. While a handful of these reports used ≈10 min of UV exposure, [47] all others used UV or heating times measured in hours. Therefore, none of these studies demonstrated membrane modification in the ultra-fast time scales needed for roll-to-roll manufacture and scale up. Furthermore, none of these approaches are designed to accurately control the selectivity of membranes that are formed through polymer self-assembly.[44,45]

In this work, we demonstrate that thoughtful utilization of rapid thiol-ene click reactions can achieve ultra-fast and effective cross-linking of self-assembled ZAC membranes. This novel chemical approach enables us to tune membrane selectivity and ion separations in a matter of seconds, decreasing processing time by over an order of magnitude compared with both past post-processing times used with ZACs[19] and with other reports of thiol-ene post-processing of various membranes. [20,23,52] We show that the resultant membranes not only exhibit high and tunable monovalent/divalent ion selectivity, but also excellent fouling resistance. These novel membranes feature selective layers fabricated from the cross-linkable ZAC methacrylate-random-sulfobetaine methacrylate) (P(AM-r-SBMA)),[19] whose chemical structure is shown in Figure 1B. In previous work, we had used photo polymerization as a cross-linking method. This required UV exposure times >5 min to observe any change; further increases in exposure time lead to smaller pore size.^[19] The key novelty of this work is the utilization of a new cross-linking chemistry, thiolene click chemistry with a dithiol, to decrease the UV exposure time down to seconds. Cross-linking for only 10 seconds led to significant changes in pore size, and varying exposure time between 10 and 40 s was shown to further tune the effective pore size, salt rejections, and mono-/divalent ion selectivity. Resultant membranes exhibited high Cl⁻⁻/SO₄²⁻ selectivities compared with many state-of-the-art membranes (Table S1). These thiol-ene cross-linked ZAC membranes provide complete resistance to irreversible fouling by an oil/water emulsion or a protein solution, easily outperforming a commercial nanofiltration membrane in terms of fouling resistance. This work is a crucial step for the scalability of self-assembled crosslinked ZAC based membranes that exhibit NF-range selectivity, and offers a novel chemical approach for fast cross-linking and functionalization of related membranes for further applications in the relevant fields of water purification, wastewater treatment, bioprocessing, dye removal, and sensing.

2. Results and Discussion

2.1. Membrane Fabrication and Cross-Linking

The cross-linkable ZAC in this work was a statistical/random copolymer of sulfobetaine methacrylate (SBMA), a zwitterionic monomer, and allyl methacrylate (AM), a hydrophobic monomer featuring a C=C double bond in its side-group that can undergo thiol-ene reactions. Through a thiol-ene reaction with a dithiol, the AM units are cross-linked (Figure 1B, Figure 2). This cross-linking reaction, particularly when performed in a solvent/plasticizer that preferentially partitions into the hydrophobic domains, prevents the swelling of zwitterionic domains when immersed in water. As a result, the effective pore size of the cross-linked ZAC-based membrane in water is smaller than that of its un-cross-linked counterpart. This principle of decreasing pore size by cross-linking the hydrophobic phase was previously demonstrated by photo polymerizing the AM groups, [19] but the time scales required for this reaction were too long to be implemented in roll-to-roll manufacturing.

Activators regenerated by electron transfer atom transfer radical polymerization (ARGET-ATRP) was employed to synthesize P(AM-r-SBMA) (Figure 1B).^[19] The lower reactivity of allyl groups in this controlled polymerization reaction scheme allowed us to polymerize AM only through its more reactive methacrylate groups while keeping the allyl side-groups intact. This synthesis scheme is highly scalable, as ARGET-ATRP is a robust polymerization technique that enables the synthesis of designed polymers and copolymers at low temperatures without the need to remove water and protic species.^[53] More recently, novel variations of ATRP have been developed to further improve scalability.^[54] ¹H NMR confirmed the active presence of allylic double bond (δ = 5.3 ppm; δ = 5.8 ppm) in the structure of P(AM-r-SBMA) (Figure S1, Supporting Information). The

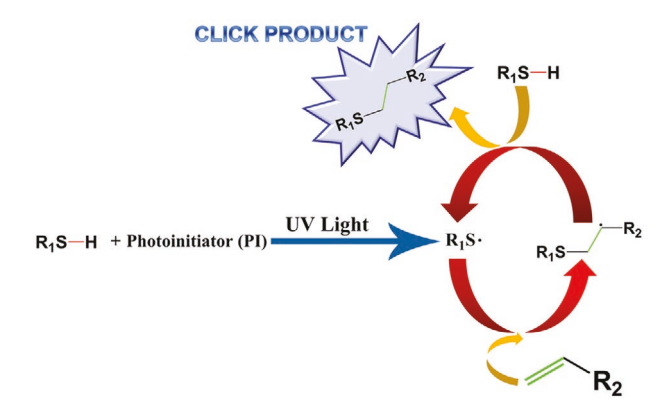


Figure 2. Schematic representation of the associated UV assisted cross-linking

overall SBMA content of the copolymer was calculated from this spectrum to be 47 wt%. This closely matches with our SBMA content in the reaction mixture. Given the relatively low conversion of 10%, the close match between copolymer and reaction mixture compositions implies a roughly random arrangement of AM and SBMA repeat units along the polymer backbone. While this low conversion was used in the presented data set to ensure the solution did not form a cross-linked gel, conversions over 50% have been achieved in subsequent experiments with similar cross-linkable copolymers containing AM and zwitterionic monomers without gelation. This indicates that this technique can be used in the future for reliable, scalable synthesis of this copolymer, without environmental impacts that significantly surpass most specialty polymer products. The prepared copolymer is a white solid, soluble in trifluoroethanol (TFE) and dimethylsulfoxide (DMSO).

The poor solubility of P(AM-r-SBMA) in common solvents limited our ability to use gel permeation chromatography (GPC) to measure its molar mass. To estimate the relative molecular weight of the copolymer, we performed dynamic light scattering (DLS) on a dilute solution of the copolymer in TFE. The copolymer showed an effective hydrodynamic radius of 60.8 ± 1 nm, corresponding to a molar mass of 2.6×10^6 g mol⁻¹ based on polyacrylonitrile standards in dimethyl formamide. It is important to mention that the molecular weight represented here is a relative value of polymer segments having a comparable hydrodynamic radius. Polymer chain aggregation and polymer-solvent interactions heavily influence the relationship between absolute molar mass and hydrodynamic radius, [55] though relative molar masses calculated by GPC also suffer from similar limitations. Therefore, this relatively high relative molar mass confirms that the synthesized copolymer is a longchain polymer.

The self-assembled nanostructured morphology of the synthesized ZAC, P(AM-r-SBMA), was characterized using TEM. The zwitterionic nanodomains were positively stained by immersion in 2% aqueous CuCl₂ for four hours to stain the zwitterionic nanodomain, as sulfobetaine groups and copper (II) ions form stable complexes.^[19,23,24,56] As seen in the bright field TEM images in **Figure 3**, P(AM-r-SBMA) self-assembles to form interconnected bicontinuous networks of hydrophobic

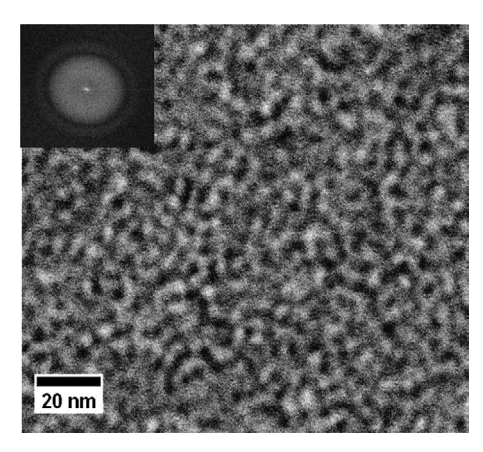


Figure 3. Bright field TEM image of self-assembled nanostructure of P(AM-*r*-SBMA). Zwitterionic domains are positively stained with Cu²⁺ ions and appear dark. Inset shows Fast Fourier transform of the image.

(bright) and zwitterionic (dark) nanodomains. The dark zwitterionic domains are interconnected, showing a percolated network through the film that allows the permeation of water. Fast Fourier Transform (FFT) analysis (Figure 3, inset) shows an average domain size of 1.4 nm. This morphology is similar to those observed for other ZACs.^[19,24]

P(AM-r-SBMA) was coated onto a commercial support membrane (Solecta, PS-35) to form a TFC membrane. For this purpose, P(AM-r-SBMA) was dissolved in TFE to form a 5 wt% solution, which was coated on top of the support by using a wire-wound metering rod. This coated membrane was placed in an oven preheated to 65 °C for 12 min. Finally, the membrane was taken out of the oven and immediately immersed in DI water overnight. This TFC membrane, as fabricated and without any cross-linking, is termed TCZ-0. Upon casting, the self-assembly of the ZAC led to the formation of a network of zwitterionic nanodomains that allow the permeation of water and solutes small enough to enter the zwitterionic nanochannels, held together by the hydrophobic AM-rich domains (Figure 3).

After the formation of these TFC membranes, the hydrophobic AM repeat units were cross-linked using a thiol-ene click reaction with a dithiol (Figure 1B). Un-cross-linked TCZ-0 membrane was soaked in a solution of IPA containing 1 wt% each of DMPA (photoinitiator) and 1,6-hexanedithiol for 10 min. Afterwards, the membrane was exposed to UV light for various time periods ranging 10–40 s. The membranes are identified as TCZ-10, TCZ-20, TCZ-30, and TCZ-40 respectively, with the last two digits specifying the UV curing time in seconds. During UV curing, DMPA acted as a photoinitiator and generated radicals on 1,6-hexanedithiol, which then reacted with the allylic double bonds of AM repeat units (Figure 2). This led to the cross-linking of the hydrophobic domains, increasing rigidity and preventing the swelling of the zwitterionic nanochannels in aqueous environments as determined by the extent of reaction.

The cross-linking of the selective layer was confirmed by analyzing the chemical composition of the selective layer using ATR-FTIR spectroscopy (**Figure 4**). Most peaks corresponding to SBMA groups and the backbone, including sharp peaks at

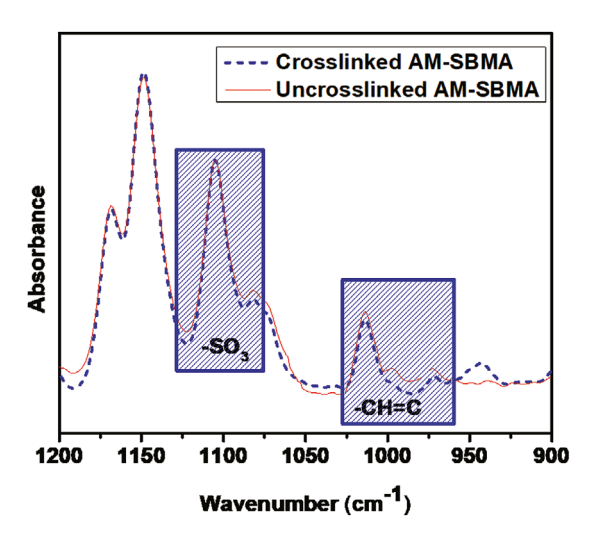


Figure 4. ATR-FTIR spectra of uncross-linked (TCZ-0) and cross-linked (TCZ-40) films of random zwitterionic copolymer P(AM-*r*-SBMA).

www.advmatinterfaces.de

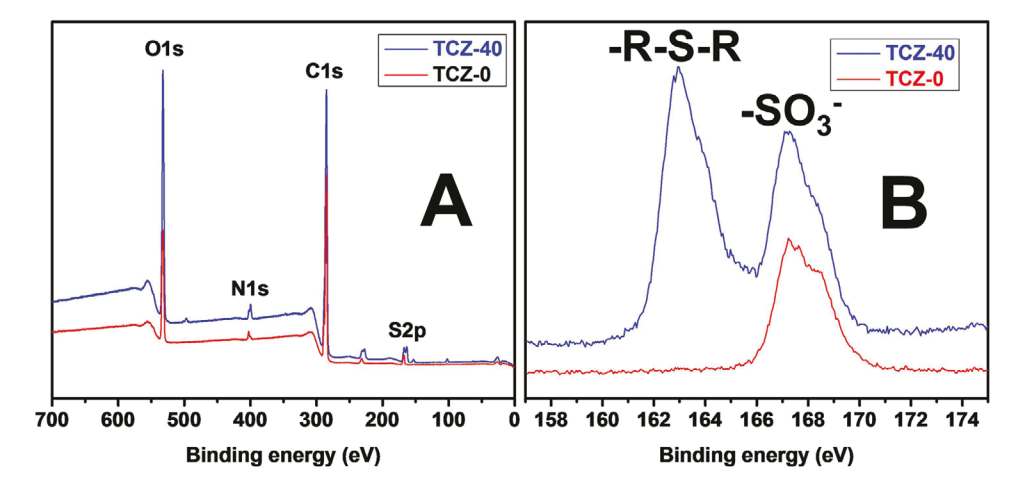


Figure 5. XPS spectra of TCZ-0 and TCZ-40 membranes. A) Survey scans, and B) high-resolution spectra for the S2p region.

≈1150 and ≈1070-1090 cm $^{-1}$ associated with C-O-C and -SO $_3$ stretching, [57,58] remained similar in both TCZ-0 and TCZ-40 membranes as expected. The main difference between the spectra was the intensity of the peak responsible for –CH=C bending (985–1004 cm $^{-1}$), [57,59] The decreased peak intensity for TCZ-40 membrane compared to TCZ-0 can be attributed to the consumption of the allyl double bonds through the thiol-ene cross-linking upon UV curing.

The surface elemental compositions of these two membranes were further characterized using XPS (Figure 5). Characteristic peaks for O1s, N1s, C1s, and S2p are present in survey spectra for both membranes (Figure 5A), in good agreement with the selective layer elemental compositions. High-resolution spectra for the S2p region (Figure 5B) allowed deeper characterization

of the binding structures around sulfur groups. The TCZ-0 membrane showed only one S2p peak (168.2 eV), arising from the SO₃ $^-$ groups on the SBMA repeat units. [60] The spectrum for the cross-linked TCZ-40 membrane exhibited two different S2p peaks, one at 163.5 eV and the other at 168.2 eV. The additional peak was associated with the thioether groups (R-S-R) formed upon the thiol-ene click reaction. [61,62] These results further confirm the expected cross-linking reaction.

The morphology of coated membranes was investigated by SEM imaging (Figure 6). A thin selective layer on top of the support membrane is clearly visible in both TCZ-0 and TCZ-40 membranes. This layer adheres to the support through partial penetration of the polymer into the fine pores of the support, forming a physical anchor, as well as through intermolecular

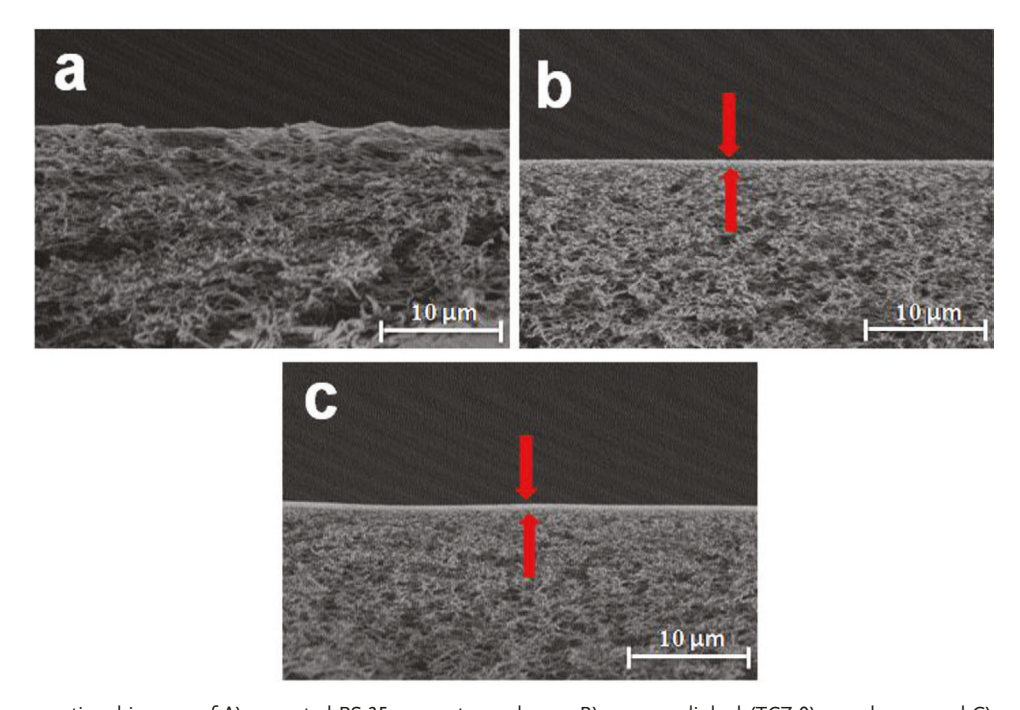


Figure 6. SEM cross-sectional images of A) uncoated PS-35 support membrane, B) un-cross-linked (TCZ-0) membrane, and C) cross-linked TCZ-40 membrane after immersion in TFE for 24 h. Cross-linking prevented the selective layer from dissolving in TFE, a solvent that readily dissolves the un-cross-linked copolymer. 7000 X magnification.

Table 1. Manufacturing conditions, permeances, and probe solute rejections for TCZ membranes with varying UV exposure times.

Name	UV exposure time [s]	Permeance [L m ⁻² .h ⁻¹ .bar ⁻¹]	VB12 rejection [%]	Riboflavin rejection [%]
TCZ-0	0	5.5 ± 0.9	$\textbf{82.1} \pm \textbf{0.3}$	32.9 ± 0.2
TCZ-10	10	3.7 ± 0.3	94.5 ± 0.2	47.3 ± 0.1
TCZ-20	20	2.3 ± 0.3	96.3 ± 0.1	54.2 ± 0.2
TCZ-30	30	1.5 ± 0.4	99.5 ± 0.1	73.5 ± 0.1
TCZ-40	40	1.2 ± 0.2	99.7 ± 0.1	74.2 ± 0.1

interactions. Upon cross-linking, there is also likely some chemical bonding between the support and the layer, as polysulfone is known to generate free radicals that can react with allyl groups in the copolymer upon UV irradiation. This layer thickness could potentially be further decreased by improving the coating processes, resulting in higher membrane permeances by up to 50 times, as demonstrated with other ZAC membrane chemistries.^[52,63]

Membrane was immersed in TFE, a solvent that readily dissolves un-cross-linked P(AM-*r*-SBMA). The fact that the selective layer is visually unchanged shows that cross-linking improves the solvent stability of this layer. This opens the door to the potential future use of cross-linked ZAC membranes in additional applications, including solvent-resistant nanofiltration and organic solvent nanofiltration (OSN).^[21,64]

2.2. Membrane Permeability and Selectivity

Membrane performance was characterized using deadend stirred cell filtration experiments (Table 1). The average permeance of the un-cross-linked TCZ-0 membrane was $5.5 \pm 0.9 \text{ L m}^{-2}.\text{h}^{-1}.\text{bar}^{-1}$. As expected from recent studies, [19,41] cross-linking of the hydrophobic domains of P(AM-r-SBMA) lead to a decrease in the effective pore size, as demonstrated by a decrease in water permeance along with an increase in the rejection of solutes. Increasing UV curing time from 10 to 40 s leads to a permeance decrease of \approx 80% compared to the un-cross-linked system (Figure 7), with the change plateauing at only \approx 30–40 s exposure time. This trend implies close to complete cross-linking of available AM groups in less than a minute, an order of magnitude less than necessary using other cross-linking chemistries such as photo polymerization of these allyl groups. [19]

One of the most crucial parameters of membranes is their selectivity. As an initial screen to characterize how UV irradiation time affected the selectivity of these membranes, we used two neutral small-molecule solutes, vitamin B12 (VB12; Stokes diameter 1.48 nm) and riboflavin (Stokes diameter ≈ 1 nm), [19] as probes. The rejections of vitamin B12 and riboflavin by the TCZ-0 membrane were 82% and 33%, respectively, consistent with previous studies. [19] The rejections of both solutes increased with increasing exposure time, stabilizing once again after 30–40 s, consistent with the permeance results (Table 1).

Previous studies indicate that the selectivity of un-crosslinked ZAC membranes is dominated by solute size.^[23,24] As the synthesized zwitterionic copolymer is electrostatically

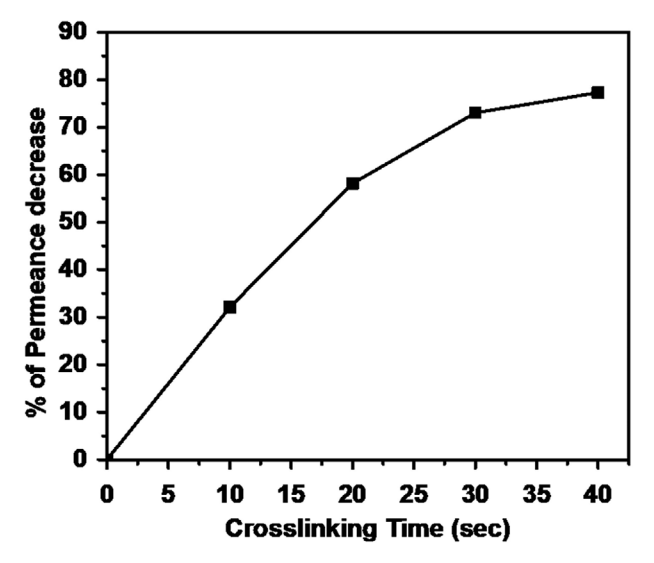


Figure 7. Effect of cross-linking time on membrane permeance decrease.

neutral, membrane selectivity is not heavily affected by solute charge, with charged and neutral solutes of roughly similar geometry sharing a rejection curve along with low salt rejections. To characterize the size-based selectivity of TCZ-0 and TCZ-40 membranes, we measured the rejection of various negatively charged dyes used in previous studies (Table 2). We should note that the calculated diameters that were used here are not Stokes diameters, but an estimate of molecular size calculated from molecular volume, acquired using Molecular Modelling Pro software. This measure is an underestimate of the actual Stokes diameters as it does not account for hydration or molecular geometry effects, but it has proven to be reliable and predictive of rejection properties of solutes by ZAC-based membranes.^[20,23,24]

Figure 8A shows the rejection of different anionic dyes by TCZ-0 and TCZ-40 membranes. The rejection of different anionic dyes with varying charges fit into a single rejection curve for both the membrane TCZ-0 and TCZ-40 (Figure 8A), implying limited charge effects as discussed earlier. The TCZ-40 membrane rejects all dyes to a higher extent than TCZ-0 does, further confirming the decrease in effective pore size. The final rejections of these dyes are all above 85%, implying very small pores that may potentially exhibit salt rejection based on steric effects and also zwitterion-ion interactions.

Table 2. Name, size, charge, and absorbance wavelength of the anionic dyes used in the filtration experiments.

Solute Name	Calculated diameter [nm]	Charge	λ [nm]
Brilliant blue R	1.11	-1	553
Direct red 80	1.08	-6	528
Chicago sky blue 6B	0.88	-4	593
Acid blue 45	0.84	-2	595
Ethyl orange	0.82	-1	474
Methyl orange	0.79	-1	463

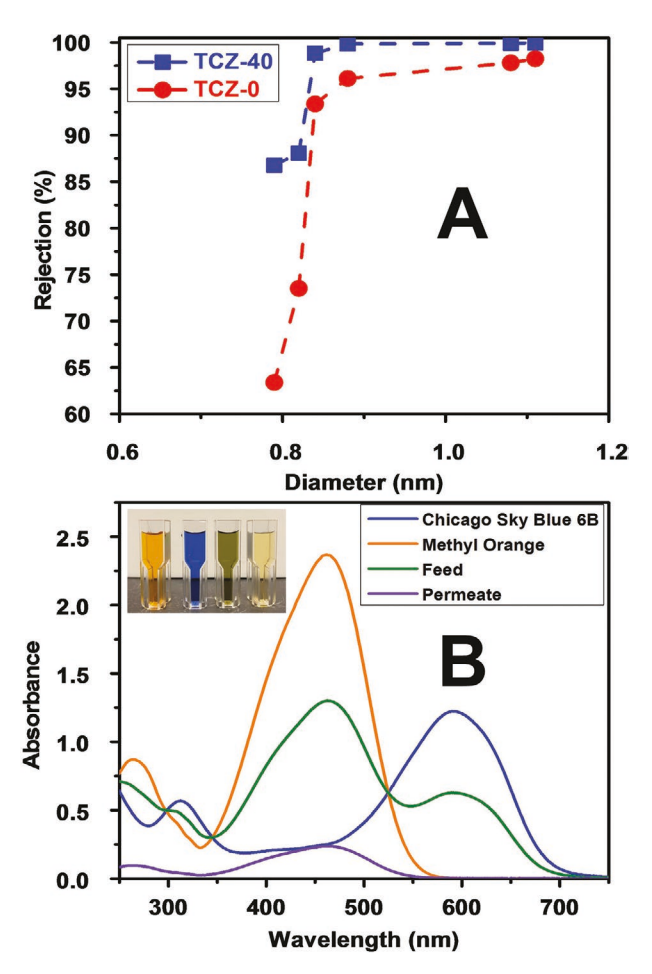


Figure 8. A) The rejection of anionic dyes of varying sizes by TCZ-0 (un-cross-linked) and TCZ-40 (cross-linked) membranes. Both membranes showed a sharp size cut-off. Cross-linked membrane showed higher rejections than the un-cross-linked one, confirming that cross-linking leads to smaller effective pore size. B) Fractionation of two dyes, Chicago sky blue 6B (0.88 nm) and methyl orange (0.79 nm), by TCZ-40, documented by the UV spectra of the feed, permeate, and each dye for reference. Only methyl orange permeates through the TCZ-40 membrane, while Chicago sky blue 6B was completely retained.

To demonstrate the ability of the TCZ-40 membrane to separate dye mixtures, we filtered a solution containing a mixture of two dyes, Chicago Sky Blue 6B (0.88 nm) and methyl orange

(0.79 nm), at the same concentration (0.05 mM). The obtained permeate contained no Chicago Sky Blue 6B, documented by the UV–visible spectrum lacking the characteristic peak of this dye at 597 nm (Figure 8B). Methyl orange still permeated through the membrane, demonstrating the fractionation of this mixture.

We tested the stability of these membranes in strong acids and bases, often used for chemical cleanings. The permeance and Vitamin B12 rejection of one of the thiol-ene cross-linked ZAC membranes, TCZ-20, did not change measurably after immersion in either 0.5 M NaOH or 0.5 M HCl for 24 hours (Supporting Information). This confirms the chemical stability of these selective layers.

As mentioned earlier, rejections of even the smallest probe dyes by TCZ-40 are quite high. This implies extremely small pores that may exhibition selectivity. As discussed in a recent study, membranes with highly cross-linked ZAC selective layers exhibit anion selectivity associated with steric effects as well as zwitterion-ion interactions.[19,41] Therefore, it is reasonable to expect selectivity between salt ions in the thiol-ene cross-linked membranes discussed here. To test this hypothesis, we measured the rejection of various salts, specifically NaCl, MgSO₄, and Na₂SO₄, using 20 mM solutions at 2-4 bar transmembrane pressure (Figure 9). Un-cross-linked TCZ-0 membrane exhibited very low salt rejection (<20% for all salts) and separation factors very close to 1 (Table S2, Supporting Information), consistent with previous un-cross-linked ZAC membranes.[19] UV curing led to increased rejection of all four salts, though the patterns in these changes depended on the nature of each salt. In as little as 10 s UV exposure, we observed significant increases to salt rejection due to cross-linking. Such rapid tuning of selectivity is unique to this system, enabled by the high reaction rates in thiol-ene chemistry as well as the unique separation mechanisms in ZAC-based membranes.

The most significant change for the shortest time periods was for Na_2SO_4 , whose rejection at 2 bars increased from ~4% to ~70% upon only 10 s of exposure. Na_2SO_4 rejection did not increase as prominently with further cross-linking, with 78% rejection after 40 s. Interestingly, the rejection of Na_2SO_4 was consistently higher than that of $MgSO_4$, though this difference was more pronounced for the shortest exposure times of 10 and 20 s. $MgSO_4$ rejection also increased more gradually, and comparatively stabilized after 30–40 s, similar to the trends for permeance and organic solute rejections. While we are still

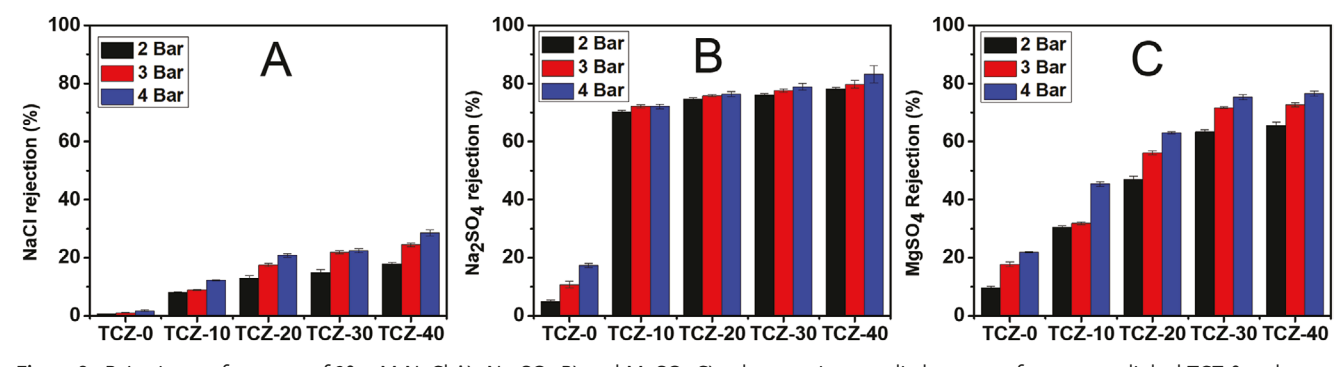


Figure 9. Rejection performance of 20 mM NaCl A), Na₂SO₄ B) and MgSO₄ C) salts at various applied pressure for un-cross-linked TCZ-0 and cross-linked TCZ membranes.





www.advmatinterfaces.de

investigating the mechanisms of ion rejection and selectivity in ZAC systems, our previous work indicates that it involves a combination of effects. Size-based selectivity is a contributor to these trends, but the fact that cross-linked ZAC membranes can, under some circumstances, exhibit selectivity between ions of similar charge and size implies zwitterion-ion interactions also play a significant role. In other words, both the size of ions and their affinity to SBMA affect selectivity. [41] In this case, the difference in trends may arise from differences in cation partitioning into the zwitterionic nanochannels, which also affects sulfate permeability due to electroneutrality. At higher degrees of cross-linking, magnesium rejection increases due to size exclusion. However, we still need extensive additional analysis and a better understanding of transport in these self-assembled systems to test this hypothesis.

The rejection of NaCl increased much less substantially with cross-linking time than the rejection of Na₂SO₄ and MgSO₄, reaching a maximum of 29% after 40 s of cross-linking. As a result, the NaCl/Na₂SO₄ separation factor increased with increasing irradiation time (Table S2, Supporting Information). The largest jump was observed within 10 s, with the separation factor mostly plateauing by 40 s. As a result, these thiol-ene cross-linked membranes have highly tunable mono-/divalent ion selectivity along with rapid and facile fabrication. For instance, membranes cross-linked for shorter times (e.g., TCZ-10) may remove divalent anions with limited cation separation, whereas highly cross-linked membranes (e.g., TCZ-40) can be used to selectively remove all divalent ions with comparatively low NaCl rejection.

2.3. Fouling Resistance

Fouling, associated with the adsorption and accumulation of feed components on the membrane surface, is one of the most significant barriers that prevent the broader use of membranes in many applications. Therefore, novel membranes should resist fouling by preventing the adsorption of organic foulants on their surface. ZAC membranes have proven to exhibit unmatched fouling resistance due to the presence of highly hydrated zwitterionic groups covering their surfaces.^[65]

We tested the resistance of these thiol-ene cross-linked ZAC membranes to fouling by various foulants. A commercial state-of-the-art nanofiltration membrane (NP-30) was also used as a benchmark to compare the fouling data with our cross-linked membrane.

We performed a static fouling experiment, which involved immersing both a thiol-ene cross-linked ZAC membrane, TCZ-40, in a solution of the protein bovine serum albumin (BSA) in phosphate buffer saline (PBS). BSA is frequently used for testing the fouling propensity of membranes due to its tendency to easily adsorb on surfaces. After 24 h in this solution, the membranes were removed and rinsed with DI water. Then, the proteins adsorbed on the membranes were stained using Gelcode Blue Safe Protein Stain. The darker blue color on the fouled NP30 membrane indicated significant protein adsorption, whereas little if any blue staining was observed on the TCZ-40 membrane (Figure S3, Supporting Information). This indicated that the cross-linked ZAC membrane TCZ-40 experi-

enced minimal if any protein fouling, outperforming the commercial membrane in terms of fouling resistance, even in this simplified system.

While the static fouling experiment is promising, membrane fouling during operation is much more complex. Fouling can occur with a broad range of chemical species depending on the feed, and concentration polarization and hydrodynamics during filtration further enhance fouling propensity. Therefore, the majority of our fouling analysis utilized dead-end stirred cell filtration experiments, often considered a worst-case scenario for fouling due to the progressive accumulation of the foulant in the filtration cell. We also screened multiple foulants.

The first foulant selected was an oil-in-water emulsion. An enormous amount of oily wastewater is regularly produced by the oil and gas industry in the form of produced water, frac water, and refinery wastewater. Proper disposal of these wastewater streams remains a critical issue. [66] Therefore, we challenged two of our cross-linked membranes (TCZ-30 and TCZ-40) with 1.5 g/L oil-in-water emulsions with a 9:1 ratio of soybean oil to DC193 surfactant, selected to represent such oily wastewater streams. [67]

Figure 10 shows data from oil-in-water emulsion fouling experiments performed in dead-end stirred cell filtration mode for TCZ-30 (Figure 10A), TCZ-40 (Figure 10B) and the commercial nanofiltration membrane NP-30 (Figure 10C). In each case, after filtering deionized water to determine the initial pure water permeance, the foulant solution was filtered for 20 h. Then, the filtration cell and membrane were rinsed several times with water, simulating physical cleaning by a forward flush with clean water. Then, pure water permeance was measured again to determine the reversibility of any fouling. All three membranes exhibited high removal of oil droplets, as indicated by the appearance of the feed and the permeate. While the feed was translucent and greyish due to light scattering by the droplets, the permeate was clear. Figure 10A (inset) demonstrates this for the TCZ-30 membrane. Permeates from the other three membranes were similar.

During the fouling experiments, both TCZ-30 and TCZ-40 membranes showed no significant decline in flux even during foulant filtration. After the water rinse, the pure water flux remains identical to the initial value. This performance is exceptional, as most membranes show at least some flux decline during the filtration step. The data obtained from the commercial NP-30 membrane (Figure 10C) is more representative of the state-of-the art. This membrane fouled significantly, losing almost \approx 48% of its initial flux during foulant filtration. This loss was not reversible through a physical cleaning process.

We also performed fouling experiments with two feeds that included BSA. The fouling potential of BSA and other proteins heavily depends on the solution properties, including ionic strength and pH. $^{[68]}$ Therefore, we prepared 1 g L $^{-1}$ solution in BSA in two different matrices. The first involved BSA dissolved in PBS (phosphate buffered saline), a quite common system for initial fouling screening in the literature. As an additional challenge, we prepared a 1 g/L solution of BSA in 10 mM CaCl $_2$ (pH: 6.4). Calcium ions have a tendency to form gels through complexation with multiple anions, leading to a high fouling propensity of the solution. $^{[69,70]}$

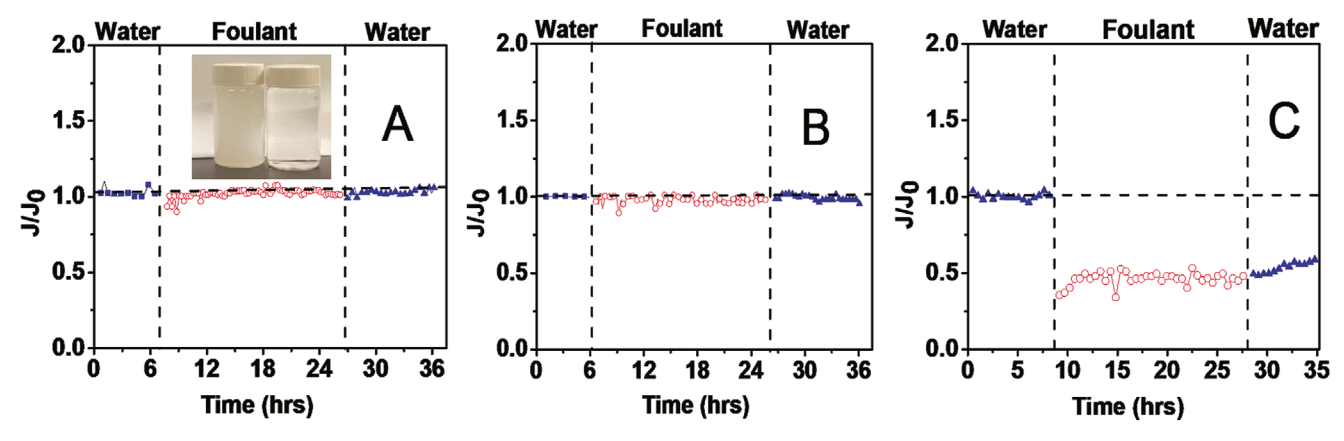


Figure 10. Dead-end fouling data with oil-in-water emulsion solutions for A) TCZ-30, B) TCZ-40, and C) a commercial membrane NP-30. The plots show the change in the normalized flux, defined as the ratio of flux at the given time point (J) normalized by the initial pure water flux (J₀). After stabilization of the initial water flux (blue), normalized flux during the filtration of the foulant solution is monitored (red). Then, the membrane is rinsed with water several times, and normalized water flux is measured again (blue). TCZ-30 and TCZ-40 membranes show no flux loss during and after exposure to foulant solutions, whereas the commercial membrane shows significant (\approx 48%) irreversible flux loss. The foulant solution was composed of 1500 mg L⁻¹ oil-in-water emulsion (9:1 oil:DC193 surfactant). Image (inset left) shows the feed (left) that is grey in colour and permeate (right) that appears clear, indicating retention of oil droplets components. J₀ = 2.75 L m⁻² hr⁻¹ for all three membranes.

Figure 11 shows the dead-end filtration of 1 g L⁻¹ of BSA protein in PBS by TCZ-30 (A) and TCZ-40 (B). The foulant solution was filtered through both the membranes for 18 h. No decline in the flux was observed during foulant filtration for either membrane. No irreversible flux loss was measured after a gentle water rinse. This phenomenon clearly shows the exceptional fouling resistance of these ZAC membranes.

In addition, we also studied the fouling of these membranes using a more challenging protein solution as described above, 1 g $\rm L^{-1}$ of BSA in 10 mM $\rm CaCl_2$ solution for 20 h (Figure 12). The TCZ-40 membrane showed negligible flux decrease during foulant filtration over 20 h, which was completely recovered after a simple water rinse. In contrast, commercial NP-30 showed almost 27% of its initial flux decline during foulant filtration. This irreversible flux loss was not recovered after the water rinse.

These experiments demonstrate the exceptional degree of fouling resistance this new family of membranes exhibits, even with challenging feeds. Any minimal membrane flux loss during foulant filtration can be easily recovered by physical

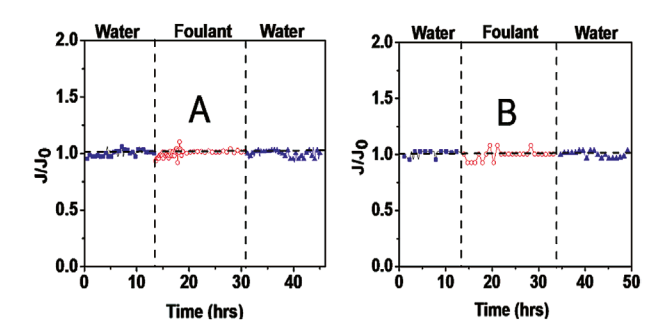


Figure 11. Fouling of A) TCZ-30 and B) TCZ-40 membranes by 1 g L⁻¹ BSA in PBS, demonstrated by the change in normalized water flux during foulant filtration (red) and after rinsing with water (blue). Both TCZ-30 and TCZ-40 membranes exhibit negligible flux loss during and after exposure to foulant solutions. $J_0 = 2.75$ L m⁻² hr⁻¹

cleaning, i.e., rinsing with water. This degree of fouling resistance, where membrane flux is mostly retained even during the dead-end filtration of highly fouling feeds, has only been matched by other ZAC-based membranes, greatly surpassing the state-of-the-art.

3. Conclusions

We have developed a new, ultra-fast cross-linking approach for tuning the selectivity of specially synthesized ZAC membranes that brought the reaction time from tens of minutes down to the order of seconds (10–40 s), utilizing thiol-ene click chemistry. This method enables the fast, scalable manufacture of highly cross-linked ZAC membranes by bringing the required UV exposure time to values accessible in roll-to-roll industrial scale manufacturing. To our knowledge, this is the first report demonstrating the use of thiol-ene click chemistry to alter the pore diameter of a self-assembled nanofiltration membrane. The ion selectivity of these membranes was tunable by varying the UV exposure time between 10 and 40 s, with longer

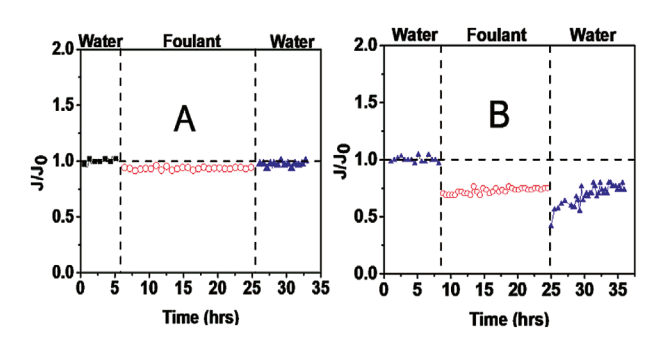


Figure 12. Fouling of A) TCZ-40 and B) NP-30 membranes by 1 g L⁻¹ BSA in 10 mM CaCl₂ solution. TCZ-40 membrane exhibited negligible flux loss during and after exposure to foulant solutions, whereas the commercial membrane showed significant (\approx 27%) irreversible flux loss. $J_0 = 2.75$ L m⁻² hr⁻¹





www.advmatinterfaces.de

exposures leading to increased ion and small molecule rejection. The longest exposure times led to high Mg²⁺ and SO₄²⁻ removal with modest NaCl rejection, whereas intermediate reaction times had high Na2SO4 rejection with lower NaCl and MgSO₄ rejections. However, the change was most drastic between 0 and 10 s, indicating a large extent of reaction even at this short time scale. Cross-linked membranes also exhibited excellent fouling resistance, the degree of which was matched only by previously developed ZAC-based membranes. No irreversible flux loss was observed during protein (BSA) or oil/ water emulsion filtration, and flux was either completely or almost completely retained even during the dead-end filtration of each foulant solution. The combination of tunable selectivity, excellent fouling resistance, ultra-fast processing, and scalability of these membranes make them promising for a wide range of applications in different industries, including biomolecule separations, textile wastewater treatment, water softening, and sulfate removal.

4. Experimental Section

Materials: Sulfobetaine methacrylate (SBMA, 95%), 2,2-Dimethoxy-2-phenylacetophenone (DMPA, 99%), 1,6-Hexanedithiol α -ethyl bromoisobutyrate (EBIB, 98%), CuBr₂ (99%), N,N,N',N'',N''pentamethyldiethylenetriamine (PMDETA, 99%), Sodium sulphate, Brilliant blue R, Direct red 80, Chicago sky blue 6B, Acid blue 45, Methyl orange, Ethyl orange and activated aluminum oxide (basic, Brockmann I, standard grade) were purchased from Sigma-Aldrich. Allyl methacrylate (AM, ≥98.0%), methanol (>99.8%), acetonitrile (≥99.5%), isopropyl alcohol (IPA, 99.5%), trifluoroethanol (TFE, ≥99.0%) sodium chloride (ACS certified), ethanol and riboflavin (98%), were purchased from Fisher Scientific. Vitamin B12 was purchased from MP Biomedicals. Hexane (>98.5% n-hexane and mixed C6-isomers) was obtained from VWR. d6- DMSO (99.5%) was purchased from Cambridge Isotope Laboratories Inc. Ascorbic acid was purchased from G-Biosciences. Commercial nanofiltration membrane NP-30 (permeance: 1.75 L/m².h.bar) was obtained from Sterlitech. PS-35, the ultrafiltration support membrane, was obtained from Solecta membranes.

Synthesis of P(AM-r-SBMA) Copolymer: AM (60 g), SBMA (40 g), and EBIB (1.55 mmol) were first mixed with 750 mL of 1:1 acetonitrile:methanol in a 2000 mL three neck round bottom flask. The mixture was purged with nitrogen to remove oxygen. Separately, a solution of 1:1 acetonitrile:methanol (50 mL) containing CuBr₂ (0.0614 mmol), ascorbic acid (0.619 mmol) and PMDETA (0.619 mmol) was prepared and purged with nitrogen. The reaction was initiated when this solution was transferred to the previously stirred solution of monomer and EBIB using a cannula. After this addition of the catalyst solution to the monomer mixture, the reaction mixture turned light blue. The reaction was carried out for 20 h at room temperature, after which the reaction was terminated by exposure to air. A rotary evaporator was then used to concentrate the polymer solution. The polymer was then precipitated in a 5:3 v/v mixture of hexane:ethanol. The obtained polymer was re-dissolved in 1:1 acetonitrile:methanol and re-precipitated in the hexane:ethanol mixture for three successive times. The polymer was then washed with hexane and dried at ambient temperature under vacuum for three days. The obtained copolymer was characterized by ¹H NMR and IR spectroscopy (Figure S1 and S2 in supporting information).

Fabrication of Un-Cross-Linked Thin Film Composite Membranes: The P(AM-r-SBMA) copolymer was first dissolved in TFE (5 wt%) at room temperature and passed successively through 1.2 μ m Titan3 glass microfiber and 0.45 μ m PTFE syringe filters (ThermoScientific). The obtained polymer solution was degassed overnight in a sealed vial prior to the coating of the selective layer. A commercial ultrafiltration support membrane (PS-35 from Solecta) was taped on top of a glass plate.

The polymer solution was coated onto the support membrane using a wire-wound metering rod (Gardco, #8, wet film thickness 20 μm). Immediately after coating, the glass plate was placed in a pre-heated oven (65 °C) for 12 min. The dried TFC membrane (TCZ-0) was then immediately immersed in DI water overnight.

Fabrication of Cross-linked Thin Film Composite Membranes: Cross-linking of the membrane (TCZ-0) was performed through UV-assisted thiol-ene click chemistry. TCZ-0 membrane coated with P(AM-r-SBMA) copolymer was first soaked in a solution of IPA (20 mL) containing 1 wt% each of 1,6-hexanedithiol and DMPA for 10 min. The soaking was done to saturate the hydrophobic domain with photoinitiator and thiol. Then, most of the solution (=90%) was taken out from the glass container and the membrane with a remaining solution was subjected to immediate UV curing (365 nm, 9 W bulb⁻¹, and four bulbs) for different times scales ranging 10–40 s. After UV curing, the membrane was removed from the glass container and cleaned extensively with IPA and DI water. Finally, cleaned membranes were stored in DI water prior to any experiments.

Membrane Characterization: Membrane was characterized using attenuated total reflectance Fourier transform infrared (ATR-FTIR) spectroscopy, scanning electron microscopy (SEM), transmission electron microscopy (TEM), and X-ray photoelectron spectroscopy (XPS). The details of these characterization techniques are provided in SI.

Membrane Testing: Membrane filtration experiments were conducted on 4.1 cm² membrane disks using a 10 mL Amicon 8010 stirred, dead-end filtration cell (Millipore), attached to a 1 gal reservoir. The weight of the permeate was monitored through an electronic scale (Ohaus Scout Pro) connected to a computer. Membrane permeance (L_p) was determined by $L_p = J/\Delta P$, where J is the volumetric flux of permeate and ΔP is the applied trans-membrane pressure. For rejection measurements (both salts and dye), 10 mL of feed solution was loaded, filtered and discarded ≈ 2 mL of permeate, and then collected an additional permeate fraction for analysis. This was found to result in reliable and steady rejection values. Rejection (R) was determined by $R = (1 - C_P/C_F)100\%$, where C_F and C_P are the feed and permeate concentrations, respectively. For the fouling studies, we first determined initial flux, fouled the membranes for 18–20 h, and finally rinsed the membrane gently with water before measuring the final flux.

Supporting Information

Supporting Information is available from the Wiley Online Library or from the author.

Acknowledgements

A. N. M. and S. J. L. contributed equally to work. We gratefully acknowledge financial support from the National Science Foundation (NSF) under grant number CHE-1904465 and the Department of Energy grant DE-DEFE003185 (led by ZwitterCo, Inc.). The authors thank Dr. Nicki Watson at the Harvard Center for Nanoscale Systems (CNS), for collecting TEM images. Center for Nanoscale Systems (CNS), a member of the National Nanotechnology Coordinated Infrastructure Network (NNCI), was supported by the National Science Foundation under NSF award no. 1541959. We thank Solecta membranes for donating PS35 support membranes. ANM thanks Rashmi Chatterjee for her relentless help and support. A.A. thanks Chris Drover for helpful conversations regarding the potential commercial applications and scale-up processes for this technology.

Conflict of Interest

Ayse Asatekin owns a minor equity in and serves as the Senior Scientific Advisor of ZwitterCo. Inc., which was the lead institution in the DOE grant DE-DEFE003185 that partially funded this work. ZwitterCo also





holds a license from Tufts University to commercialize the technology described in this manuscript. Other authors declare no conflicting interests.

Data Availability Statement

The data that support the findings of this study are available from the corresponding author upon reasonable request.

Keywords

click chemistry, membranes, scalable manufacturing, water treatment, zwitterions

Received: December 20, 2021 Revised: February 14, 2022 Published online: March 17, 2022

- [1] E. A. Jackson, M. A. Hillmyer, ACS Nano 2010, 4, 3548.
- [2] M. Elimelech, W. A. Phillip, Science 2011, 333, 712.
- [3] I. C. Escobar, B. Van Der Bruggen, J. Appl. Polym. Sci. 2015, 132, 42002.
- [4] S. R. Lewis, S. Datta, M. Gui, E. L. Coker, F. E. Huggins, S. Daunert, L. Bachas, D. Bhattacharyya, Proc. Natl. Acad. Sci. USA 2011, 108, 8577.
- [5] M. A. Shannon, P. W. Bohn, M. Elimelech, J. G. Georgiadis, B. J. Marías, A. M. Mayes, *Nature* **2008**, 452, 301.
- [6] C. Christy, S. Vermant, Desalination 2002, 147, 1.
- [7] D. R. P. G. M. Geise, H.-S. Lee, D. J. Miller, B. D. Freeman, J. E. Mcgrath, J. Polym. Sci., Part B: Polym. Phys. 2004, 48, 1685.
- [8] I. Sadeghi, P. Kaner, A. Asatekin, Chem. Mater. 2018, 30, 7328.
- [9] P. J. J. Alvarez, C. K. Chan, M. Elimelech, N. J. Halas, D. Villagrán, Nat. Nanotechnol. 2018, 13, 634.
- [10] H. B. Park, J. Kamcev, L. M. Robeson, M. Elimelech, B. D. Freeman, Science 2017, 356, 307.
- [11] J. R. Werber, C. O. Osuji, M. Elimelech, Nat. Rev. Mater. 2016, 1, 16018
- [12] E. N. Savariar, K. Krishnamoorthy, S. Thayumanavan, Nat. Nanotechnol. 2008. 3, 112.
- [13] S. B. Lee, D. T. Mitchell, L. Trofin, T. K. Nevanen, H. Söderlund, C. R. Martin, *Science* **2002**, *296*, 2198.
- [14] B. B. Lakshmi, C. R. Martin, Nature 1997, 388, 758.
- [15] A. Alsbaiee, B. J. Smith, L. Xiao, Y. Ling, D. E. Helbling, W. R. Dichtel, *Nature* **2016**, *529*, 190.
- [16] R. Van Reis, A. Zydney, Curr. Opin. Biotechnol. 2001, 12, 208.
- [17] A. Kalbasi, L. Cisneros-Zevallos, J. Agric. Food Chem. 2007, 55, 7036.
- [18] N. Hilal, O. O. Ogunbiyi, N. J. Miles, R. Nigmatullin, Sep. Sci. Technol. 2005, 40, 1957.
- [19] S. J. Lounder, A. Asatekin, Chem. Mater. 2021, 33, 4408.
- [20] P. Bengani-Lutz, R. D. Zaf, P. Z. Culfaz-Emecen, A. Asatekin, J. Membr. Sci. 2017, 543, 184.
- [21] P. Marchetti, M. F. Jimenez Solomon, G. Szekely, A. G. Livingston, Chem. Rev. 2014, 114, 10735.
- [22] M. Moslehi, H. Mahdavi, A. Ghaffari, J. Polym. Environ. 2021, 29, 2463.
- [23] P. Bengani-Lutz, E. Converse, P. Cebe, A. Asatekin, ACS Appl. Mater. Interfaces 2017, 9, 20859.
- [24] P. Bengani, Y. Kou, A. Asatekin, J. Membr. Sci. 2015, 493, 755.
- [25] K. V. Peinemann, V. Abetz, P. F. W. Simon, Nat. Mater. 2007, 6, 992.
- [26] A. Asatekin, A. Menniti, S. Kang, M. Elimelech, E. Morgenroth, A. M. Mayes, J. Membr. Sci. 2006, 285, 81.

- [27] S. Y. Yang, I. Ryu, H. Y. Kim, J. K. Kim, S. K. Jang, T. P. Russell, Adv. Mater. 2006, 18, 709.
- [28] Y. Zhang, N. E. Almodovar-Arbelo, J. L. Weidman, D. S. Corti, B. W. Boudouris, W. A. Phillip, npj Clean Water 2018, 1, 1.
- [29] R. Shevate, M. Karunakaran, M. Kumar, K. V. Peinemann, J. Membr. Sci. 2016, 501, 161.
- [30] A. Asatekin, E. A. Olivetti, A. M. Mayes, J. Membr. Sci. 2009, 332, 6.
- [31] A. Akthakul, R. F. Salinaro, A. M. Mayes, Macromolecules 2004, 37, 7663
- [32] D. L. Gin, W. Gu, B. A. Pindzola, W. J. Zhou, Acc. Chem. Res. 2001, 34, 973.
- [33] M. Zhou, T. J. Kidd, R. D. Noble, D. L. Gin, Adv. Mater. 2005, 17, 1850
- [34] Q. Yang, M. Ulbricht, Chem. Mater. 2012, 24, 2943.
- [35] S. Chen, S. Jiang, Adv. Mater. 2008, 20, 335.
- [36] M. Herzberg, A. Sweity, M. Brami, Y. Kaufman, V. Freger, G. Oron, S. Belfer, R. Kasher, Biomacromolecules 2011, 12, 1169.
- [37] R. Yang, J. Xu, G. Ozaydin-Ince, S. Y. Wong, K. K. Gleason, Chem. Mater. 2011, 23, 1263.
- [38] Y. L. Ji, Q. F. An, Q. Zhao, W. D. Sun, K. R. Lee, H. L. Chen, C. I. Gao, I. Membr. Sci. 2012, 243, 390.
- [39] T. Wu, F. L. Beyer, R. H. Brown, R. B. Moore, T. E. Long, *Macromolecules* 2011, 44, 8056.
- [40] S. A. Sulfopropyl, C. S. Studies, M. Ehrmann, A. Mathis, B. Meurer, M. Scheer, J. Galin, I. C. S. Crm-eahp, *Macromolecules* 1992, 25, 2253
- [41] S. J. Lounder, A. Asatekin, Proc. Natl. Acad. Sci. USA 2021, 118, e2022198118.
- [42] S. Qu, T. Dilenschneider, W. A. Phillip, ACS Appl. Mater. Interfaces 2015, 7, 19746.
- [43] C. Liu, J. Lee, J. Ma, M. Elimelech, Environ. Sci. Technol. 2017, 51, 2161.
- [44] D. L. Shaffer, H. Jaramillo, S. Romero-Vargas Castrillón, X. Lu, M. Elimelech, J. Membr. Sci. 2015, 490, 209.
- [45] G. Kang, M. Liu, B. Lin, Y. Cao, Q. Yuan, Polymer 2007, 48, 1165.
- [46] A. B. Lowe, Polym. Chem. 2010, 1, 17.
- [47] L. Zhu, T. J. Zimudzi, N. Li, J. Pan, B. Lin, M. A. Hickner, Polym. Chem. 2016, 7, 2464.
- [48] X. Zhang, Y. Cao, M. Zhang, Y. Huang, Y. Wang, L. Liu, N. Li, J. Membr. Sci. 2020, 596, 117700.
- [49] K. Kim, P. Heo, J. Han, J. Kim, J. C. Lee, J. Power Sources 2018, 401, 20.
- [50] M. He, Q. Wang, W. Zhao, C. Zhao, J. Mater. Chem. B 2018, 6, 3904.
- [51] J. Deng, Z. Dai, L. Deng, J. Polym. Sci. 2020, 58, 2575.
- [52] P. Bengani-Lutz, I. Sadeghi, S. J. Lounder, M. J. Panzer, A. Asatekin, ACS Appl. Polym. Mater. 2019, 1, 1954.
- [53] Q. Lou, D. A. Shipp, ChemPhysChem 2012, 5810, 3257.
- [54] W. Jakubowski, Prog. Control Radic. Polym. Mech. Tech. 2012, 1100, 203.
- [55] W. Schärtl, Light Scattering from Polymer Solutions and Nanoparticle Dispersions, 1 Ed, Springer-Verlag, Berlin Heidelberg, Berlin Heidelberg, 2007.
- [56] Y. Song, E. E. Doomes, J. Prindle, R. Tittsworth, J. Hormes, C. S. S. R. Kumar, J. Phys. Chem. B 2005, 109, 9330.
- [57] R. M. Silverstein, F. X. Webster, D. J. Kiemle, Spectrometric Identification of Organic Compounds, John Wiley Sons, Inc., New York 2005, 7th Ed.
- [58] A. N. Mondal, B. P. Tripathi, V. K. Shahi, J. Mater. Chem. 2011, 21, 4117.
- [59] T. K. Vardareli, S. Keskin, A. Usanmaz, J. Macromol. Sci. Part A: Pure Appl. Chem. 2008, 45, 302.
- [60] S. E. Gomez-Gonzalez, G. G. Carbajal-Arizaga, R. Manriquez-Gonzalez, W. De, L.a Cruz-Hernandez, S. Gomez-Salazar, Mater. Res. Bull. 2014. 59, 394.
- [61] A. N. Mondal, Y. He, L. Wu, M. I. Khan, K. Emmanuel, M. M. Hossain, L. Ge, T. Xu, J. Mater. Chem. A 2017, 5, 1022.





www.advmatinterfaces.de

- [62] J. Pan, L. Zhu, J. Han, M. A. Hickner, Chem. Mater. 2015, 27, 6689.
- [63] X. Qian, T. Ravindran, S. J. Lounder, A. Asatekin, J. R. McCutcheon, J. Membr. Sci. 2021, 635, 119428.
- [64] D. Bhanushali, D. Bhattacharyya, Ann. N. Y. Acad. Sci. 2003, 177, 159.
- [65] A. V. Dudchenko, P. Bengani-lutz, A. Asatekin, M. S. Mauter, ACS Appl. Polym. Mater. 2020, 2, 4709.
- [66] A. Asatekin, A. M. Mayes, Environ. Sci. Technol. 2009, 43, 4487.
- [67] D. Wandera, S. R. Wickramasinghe, S. M. Husson, J. Membr. Sci. 2011, 373, 178.
- [68] A. Persson, A. S. Jönsson, G. Zacchi, J. Membr. Sci. 2003, 223, 11.
- [69] W. S. Ang, M. Elimelech, J. Membr. Sci. 2007, 296, 83.
- [70] S. Li, S. G. J. Heijman, J. Q. J. C. Verberk, P. L.e Clech, J. Lu, A. J. B. Kemperman, G. L. Amy, J. C. van Dijk, Water Res. 2011, 45, 6289.